CASA0002 - Final Assessment

Student Number: 2322 3333

April 20 2024

This paper explores the resilience and methodological limitations of London's Underground network. This paper evaluates the network's topological resilience by simulating the impact of removing key stations. It then incorporates passenger flows to evaluate the network's vulnerability under hypothetical changes in job availability and transport costs.

1 London's Underground Resilience: Topological Network Analysis

1.1 Centrality Measures

The concept of "Centrality" is useful for identifying key stations in the London Tube network. High centrality scores indicate stations whose failure could lead to significant disruptions in the network (Zhang et al. 2019).

This paper will leverage three centrality measures to identify London's most topologically important stations, *Betweeness, Degree* and *Closeness*. Below, we outline their equations alongside the top 10 stations by centrality score.

1.1.1 Betweeness Centrality

Betweeness measures the extent to which a node lies on the shortest path between other nodes in the network. In the context of the London Underground, it identifies stations through which the highest number of shortest paths pass through, indicating stations that are critical for maintaining connectivity across the network (Derrible 2012)(Stamos 2023).

$$C_B(v) = \sum_{s,t \neq v} \frac{\sigma_{st}(v)}{\sigma_{st}} \tag{1}$$

$\sigma_{st}(v)$ represents of the number of shortest paths from node s to node t that traverse node v. σ_{st} signifies the number of shortest paths between s and t. In the context of the Underground, v denotes a station and $\sigma_{st}(v)$ indicates the number of routes between other stations s and t that include station v (Stamos 2023).

This equation can be normalised using N to represent the total number of nodes in the network (Stamos 2023) (Ye et al. 2020):

$$C_B(v) = \frac{1}{N^2} \sum_{s,t \neq v} \frac{\sigma_{st}(v)}{\sigma_{st}} \tag{2}$$

The top 10 stations ranked by Topological Betweeness, are visualised below. In Figure 1 stations with higher centrality scores are larger and lighter coloured.

	Station Name	Normalised Top. Betweeness
1	Stratford	23768.09
2	Bank and Monument	23181.06
3	Liverpool Street	21610.39
4	King's Cross St. Pancras	20373.52
5	Waterloo	19464.88
6	Green Park	17223.62
7	Euston	16624.28
8	Westminster	16226.16
9	Baker Street	15287.11
10	Finchley Road	13173.76

Table 1: Top 10 Stations Ranked by Topological Betweeness

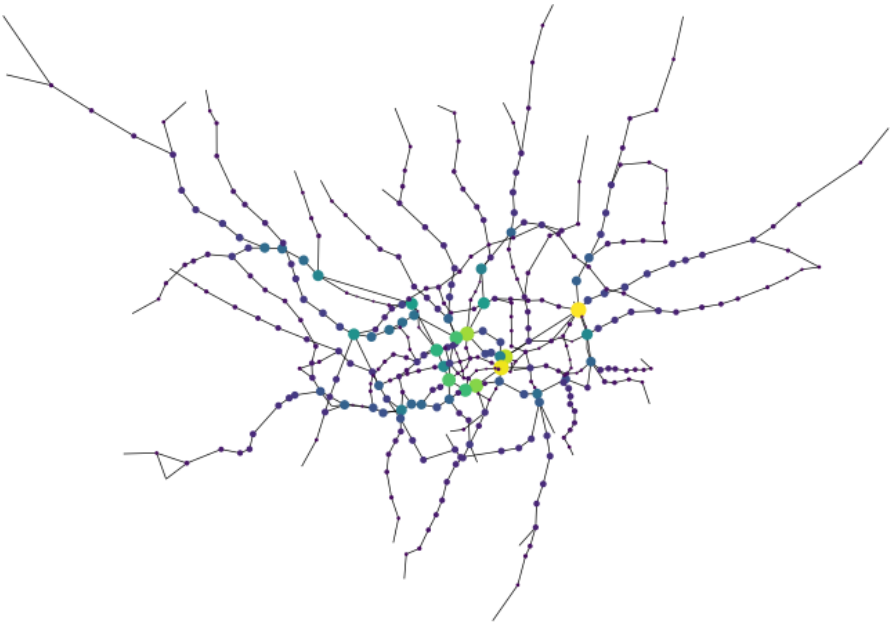

Figure 1: London Underground Network: Normalised Topological Betweeness

Stratford, Bank and Monument and Liverpool Street rank highly, indicating their significance as hubs for routing traffic between various parts of the network, likely major transfer points.

1.1.2 Degree Centrality

Degree Centrality measures the number of direct connections a node has, highlighting stations that serve as major hubs for passenger transfers (Stamos 2023) (Napitupulu et al. 2021). The non-normalised degree centrality of a node v in a network is given by the sum of its adjacency matrix entries, where $a_{v,i}$ is 1 if there is an edge between node v and node i, and 0 otherwise.

$$deg(v) = \sum_{i=1}^{N} a_{v,i} \tag{3}$$

n represents the total number of stations in the network. v represents a station, with $deg(v)$ indicating the number of lines connected to that station, normalised by $n-1$ (Stamos 2023). The normalised degree is thus:

$$C_D(v) = \frac{deg(v)}{n-1} \tag{4}$$

The top 10 stations ranked by Topological Degree:

Rank	Station Name	Normalised Top. Degree Centrality	Degree
1	Stratford	0.023	9
2	Bank and Monument	0.020	8
3	Baker Street	0.018	7
4	King's Cross St. Pancras	0.018	7
5	Green Park	0.015	6
6	Canning Town	0.015	6
7	Earl's Court	0.015	6
8	West Ham	0.015	6
9	Waterloo	0.015	6
10	Oxford Circus	0.015	6

Table 2: Top 10 London Underground Stations Ranked by Topological Degree Centrality

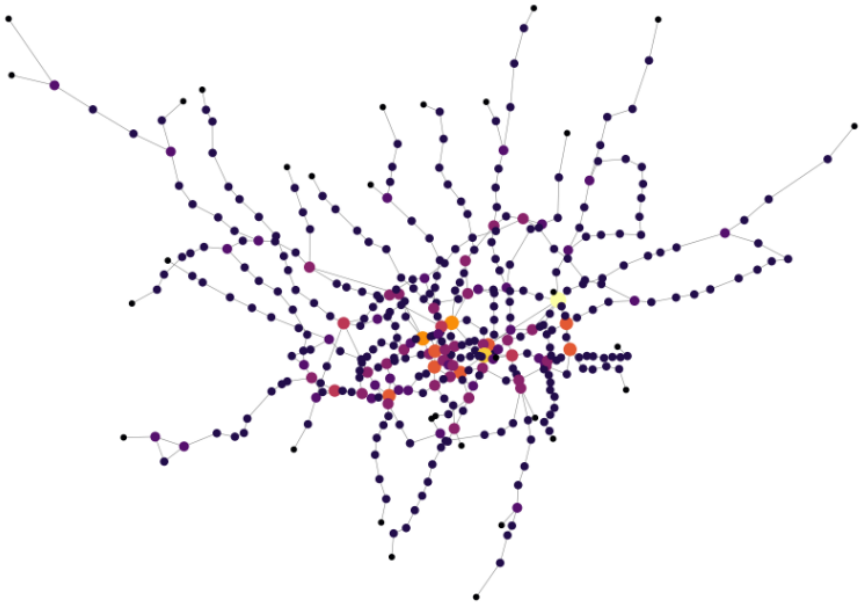

Figure 2: London Underground Network: Topological Degree Centrality

Stratford, Bank and Monument and Baker Street emerge as the stations with the highest degree centrality, indicating their importance in terms of the number of lines passing through them, likely acting as key interchange points.

1.1.3 Closeness Centrality

Closeness is a score that indicates how physically close a node is to all other nodes in the network based on edge length. It identifies stations that offer the shortest average journey time to all other stations (Stamos 2023).

$$C_i = \frac{1}{l_i} = \frac{n}{\sum_j d_{ij}} \tag{5}$$

l_i represents the average shortest path length from node i to all other nodes and d_{ij} signifies the shortest path length between nodes i and j and n again is the total number of stations. In the context of the Underground, i represents a station and l_i indicating the average distance from station i to all other stations calculated as the reciprocal of the sum of shortest path lengths (Stamos 2023).

The top 10 Stations ranked by Topological Closeness are listed below alongside a visualisation.

Rank	Station Name	Topological Closeness Centrality
1	Green Park	0.114778
2	Bank and Monument	0.113572
3	King's Cross St. Pancras	0.113443
4	Westminster	0.112549
5	Waterloo	0.112265
6	Oxford Circus	0.111204
7	Bond Street	0.110988
8	Farringdon	0.110742
9	Angel	0.110742
10	Moorgate	0.110314

Table 3: Top 10 London Underground Stations Ranked by Topological Closeness Centrality

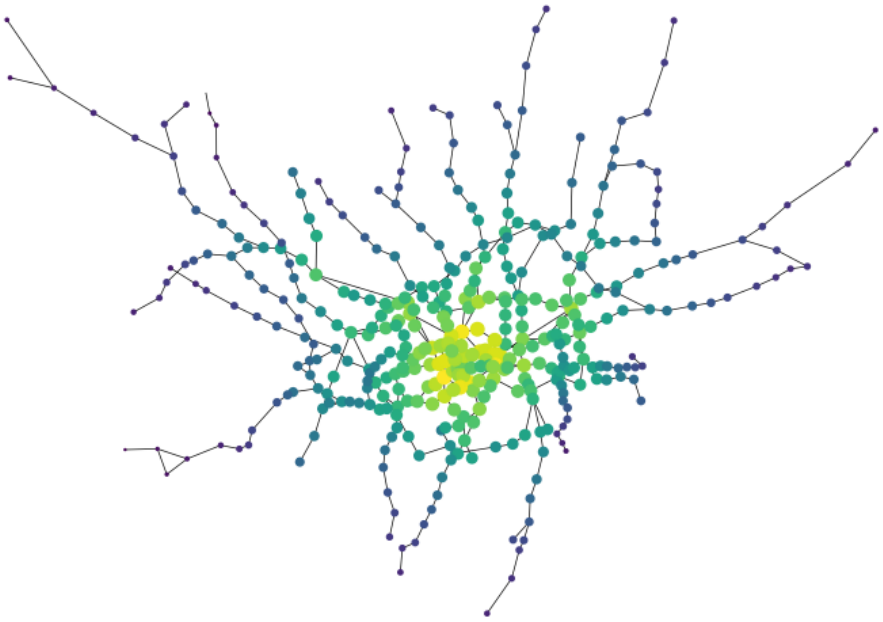

Figure 3: London Underground Network: Topological Closeness Centrality

Green Park, Bank and Monument and King's Cross St. Pancras rank highly, suggesting they are centrally located and accessible to a large number of other stations. These stations likely play a crucial role in facilitating efficient travel by providing access to various parts of the network.

1.2 Impact Measures

In section I.3 we assess which centrality measure is most effective in evaluating a station's network importance. This will be done by removing the top 10 nodes, sequentially and non-sequentially, for each topological measure.

To measure the impact each station's removal has, two impact measures will be used, *Global Efficiency* and *Average (Shortest) Path Length*. While related, together they provide a comprehensive view of network robustness, capturing direct connectivity and the resilience of alternate routing paths.

Global efficiency measures how efficiently a network facilitates information or passenger transfer among nodes.

$$E_{\text{glob}} = \frac{1}{n(n-1)} \sum_{i \neq j \in G} \frac{1}{d(i,j)}$$

This formula calculates the average of the inverse shortest path distances $d(i,j)$ between all pairs of stations i and j in the network (Latora & Marchiori

2001). n is the total number of stations, the formula includes a normalising factor $\frac{1}{n(n-1)}$ to account for each possible pair of nodes, ensuring the measure is scalable. Higher values indicate a network with better connectivity between all station pairs (Vragović et al. 2005).

Assuming an agent takes the shortest path from point i to j, the ***Average Shortest Path Length*** is the average number of steps or edges along the shortest paths for all possible pairs of nodes in a network (Latora & Marchiori 2001). When a node is removed, some paths get longer while others become unreachable if the network becomes disconnected. Higher scores mean longer average travel times for passengers, meaning the network is less efficient(Latora & Marchiori 2001).

$$L = \frac{1}{n(n-1)} \sum_{i \neq j \in G} d(i,j) \tag{6}$$

In some cases, our graph may become disconnected and Average Shortest Path Length will be unrepresentative of our entire network. If this occurs, we will calculate Average Shortest Path Length for each sub graph, then, find the weighted mean of all subgraphs. This is calculated using the following equation:

$$L_{\text{mean}} = \sum_{k=1}^{m} \frac{n_k}{n} L_k \tag{7}$$

Where:

L_{mean} : Mean of the average shortest path lengths
m : Number of subgraphs
n_k : Number of nodes in the kth subgraph
L_k : Average shortest path length of the kth subgraph
n : Total number of nodes in the entire graph

These measures are not specific to the London Underground but are general metrics applicable to any network system highlighted by their scaling factors . They assess the impact of node removals on *overall network performance*, making them useful for assessing the efficiency and robustness of all networks (Latora & Marchiori 2001).

1.3 Node Removal Analysis

We will conduct node removal using two distinct approaches: non-sequential and sequential. **Sequential Removal** removes the top node in the network based on centrality score one at a time, recalculates centrality and repeats. **Non-sequential Removal** randomly removes nodes from the top 10 station list, based on centrality score, recalculates centrality and repeats

The impact is assessed using Global Efficiency (GE) and Average Shortest Path Length (ASPL).

1.3.1 Node Removal: Topological Betweeness

Removal	Stations Removed	ASPL	GE	Largest Component
0	-	13.545998	0.101256	401
1	Stratford	14.496447	0.098215	379
2	King's Cross St. Pancras	15.310134	0.093431	378
3	Waterloo	15.795939	0.090360	377
4	Bank and Monument	16.789631	0.085753	376
5	Canada Water	19.029234	0.080369	375
6	West Hampstead	13.462360	0.108644	227
7	Earl's Court	14.206450	0.104054	226
8	Shepherd's Bush	13.792046	0.109139	196
9	Euston	13.821885	0.113125	173
10	Baker Street	18.193596	0.097561	170

Table 4: Sequential Node Removal: Topological Betweeness

Removal	Stations Removed	ASPL	GE	Largest Component
0	-	13.545998	0.101256	401
1	Bank and Monument	14.130739	0.096735	400
2	Stratford	14.872497	0.094833	378
3	Green Park	15.188498	0.092654	377
4	Finchley Road	16.063574	0.089269	376
5	Finsbury Park	16.550394	0.087551	367
6	Euston	16.641976	0.088067	344
7	West Brompton	17.095238	0.086876	336
8	London Bridge	18.306730	0.083387	335
9	West Hampstead	20.098739	0.080298	334
10	Euston Square	20.934404	0.078500	333

Table 5: Non-Sequential Node Removal: Topological Betweeness

1.3.2 Node Removal: Topological Degree

Removal	Stations Removed	ASPL	GE	Largest Component
0	-	13.545998	0.101256	401
1	Stratford	14.496447	0.098215	379
2	Bank and Monument	14.872497	0.094833	378
3	Baker Street	15.686438	0.090588	377
4	King's Cross St. Pancras	17.013376	0.084431	374
5	Earl's Court	17.375897	0.082577	373
6	Green Park	17.549923	0.081434	372
7	Canning Town	17.894731	0.080833	358
8	Turnham Green	18.317581	0.079135	357
9	Oxford Circus	18.468704	0.078279	355
10	Willesden Junction	20.259861	0.074963	336

Table 6: Sequential Node Removal: Topological Degree

Removal	Stations Removed	ASPL	GE	Largest Component
0	-	13.545998	0.101256	401
1	Green Park	13.824536	0.099190	400
2	Stratford	14.783420	0.096064	378
3	Bank and Monument	15.188498	0.092654	377
4	West Ham	15.780835	0.090891	374
5	Turnham Green	16.080861	0.089482	373
6	King's Cross St. Pancras	17.434933	0.083160	372
7	Baker Street	18.337163	0.079683	369
8	Liverpool Street	18.353956	0.079795	363
9	Oxford Circus	18.492151	0.078975	361
10	Canning Town	18.326799	0.080109	34

Table 7: Non-Sequential Node Removal: Topological Degree

1.3.3 Node Removal: Topological Closeness

Removal	Stations Removed	ASPL	GE	Largest Component
0	-	13.545998	0.101256	401
1	Green Park	13.824536	0.099190	400
2	King's Cross St. Pancras	14.658480	0.094435	399
3	Waterloo	15.114818	0.091816	398
4	Bank and Monument	16.702427	0.085426	397
5	West Hampstead	18.974696	0.080544	396
6	Canada Water	13.978014	0.104746	226
7	Stratford	13.978014	0.104746	226
8	Earl's Court	14.729722	0.100184	225
9	Shepherd's Bush	14.747608	0.103441	195
10	Oxford Circus	15.661877	0.097733	194

Table 8: Sequential Node Removal: Topological Closeness

Removal	Stations Removed	ASPL	GE	Largest Component
0	-	13.545998	0.101256	401
1	Bond Street	13.726090	0.099968	400
2	Westminster	13.923893	0.098763	399
3	Bank and Monument	14.338759	0.095101	398
4	Euston	14.602909	0.095093	375
5	Oxford Circus	14.836734	0.093614	374
6	Great Portland Street	15.694601	0.090568	373
7	Angel	15.722792	0.090362	372
8	King's Cross St. Pancras	16.218003	0.087938	370
9	Canada Water	19.267350	0.080548	369
10	Kensal Rise	20.008189	0.078960	368

Table 9: Non-Sequential Node Removal: Topological Closeness

1.3.4 Node Removal: Results and Analysis

Below, the Sequential and Non-Sequential node removal for each centrality measure is plotted against the resulting Global Efficiency and Average Shortest Path Length.

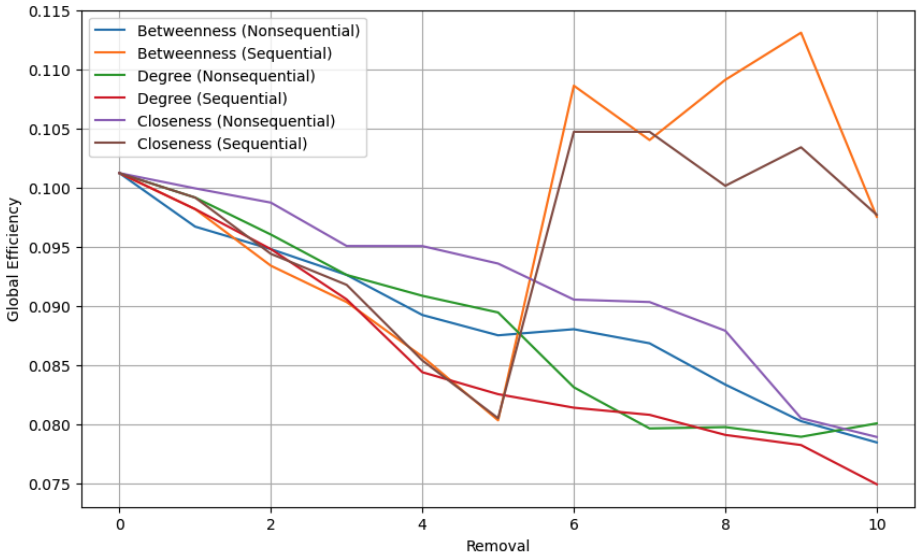

Figure 4: Impact of Node Removal on Global Efficiency

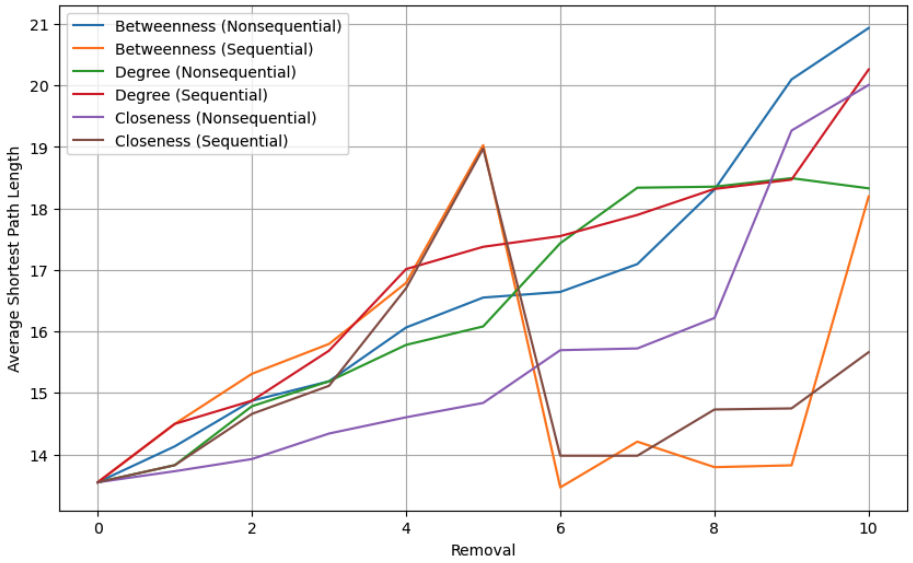

Figure 5: Impact of Node Removal on Average Shortest Path Length

Degree Node Removal shows network performance declines when key nodes are removed sequentially and non-sequentially. Average path length increases and efficiency decreases. In regards to degree centrality, the network struggles with sequential disruptions slightly more than non-sequential ones. Sequential

Betweeness and *Closeness* node removal give us sporadic results and surprisingly impact our indicators less than non-sequential removal.

Non-sequential Removal is a more effective and realistic strategy for studying resilience, It better simulates unexpected disruptions (such as accidents or random failures). Aside from a tragic London Bombings in July 2005, there have been no targeted attacks of London Underground stations while there are hundreds of unexpected station closures every year (Lucy Rodgers et al. 2015) (British Transport Police n.d.).

Below, we see node removal strategies and their impact on network connectivity. Betweeness is the most effective measure in determining the vulnerability. Sequential and Non-Sequential removal of Betweeness nodes disconnect the network most, reducing percentage of the network connected to 44% and 79%, respectively. This is a reasonable result, as it captures the role of stations as *bridges* in the network (Esposito Amideo et al. 2019).

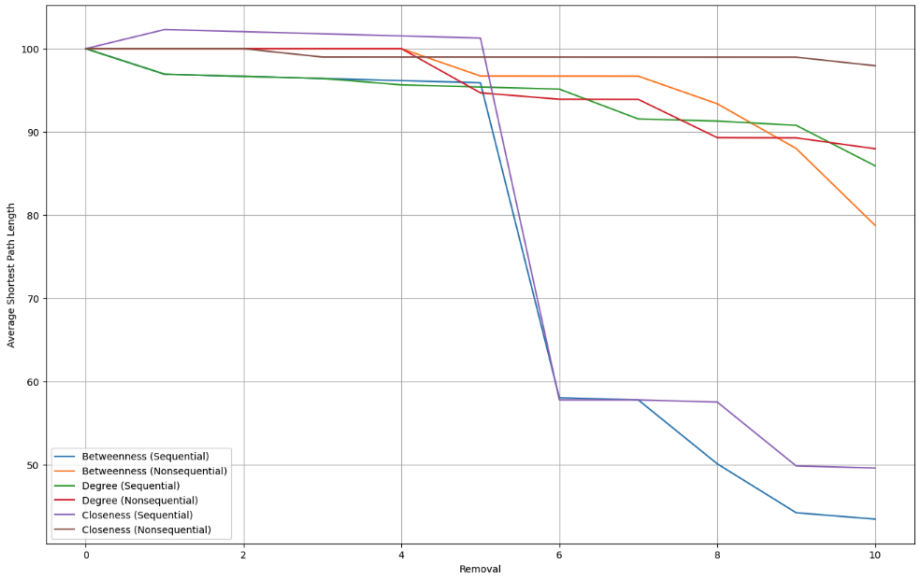

Figure 6: Percentage of Network Connected Across Different Centrality Measures

The Global Efficiency coefficient of variation is 0.580, which is lower than Average Shortest Path Length (0.643), indicating a higher stability of measure (Zhou & Wang 2018). It's R-squared value of 0.262, suggesting 26.2% of its variability is predictably explained by node removal, unlike the Average Shortest Path Length which had a significantly lower R-squared value of 0.14. This indicates that Global Efficiency responds to changes in the network in a more predictable and consistent manner, making it more reliable for assessing the impact of node removal (Zhou & Wang 2018).

2 London's Underground Resilience: Weighted Network Analysis

We build on our analysis by accounting for passenger flows. Below is the visualised flow weighted network. Thicker and lighter coloured edges indicate higher passenger flows.

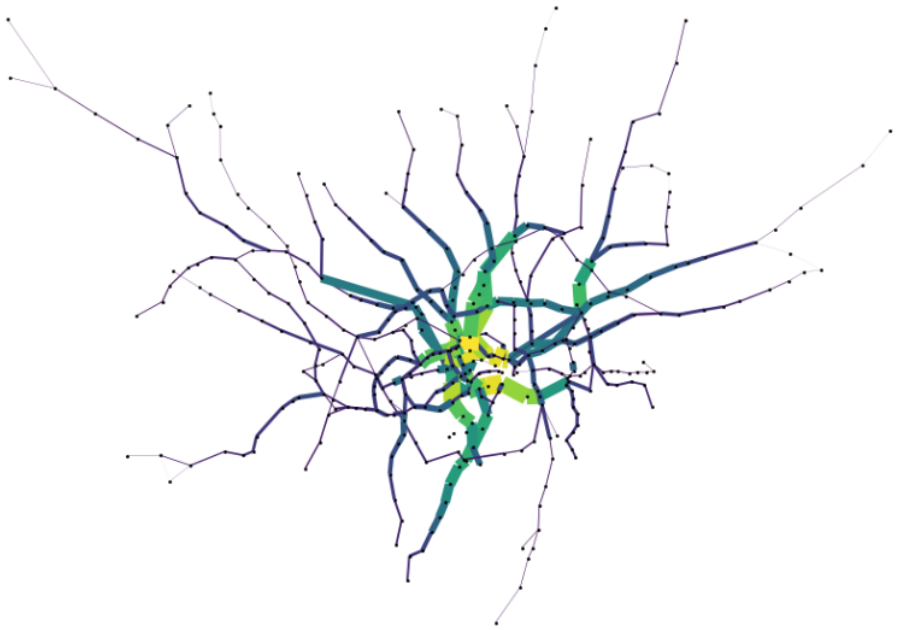

Figure 7: Passenger Flows in the London Tube

In order to calculate centrality inclusive of flows, we must change our topological equations slightly.

2.1 Betweeness Centrality inclusive of Flows and Edge Length

Flow Weighted Betweeness Centrality Equation:

$$C_{FB}(i) = \sum_{s \neq i \neq t} \frac{\text{flow}_{st}(i)}{\text{total flow}_{st}} \tag{8}$$

The standard Betweeness equation counts shortest paths through nodes, while the weighted version accounts for passenger flow along edges, using $\text{flow}_{st}(v)$ and total flow_{st}, which respectively denote the flow through node v and the total flow from node s to node t (Stamos 2023).

The top ten stations ranked by their flow Betweeness are displayed below.

Station	Flow Betweeness Centrality
Bank and Monument	0.221154
King's Cross St. Pancras	0.211320
Stratford	0.183663
Oxford Circus	0.169491
Euston	0.167125
Baker Street	0.153105
Earl's Court	0.142597
Shadwell	0.140027
South Kensington	0.129074
Waterloo	0.127000

Table 10: London Underground Network: Inclusive of Flows

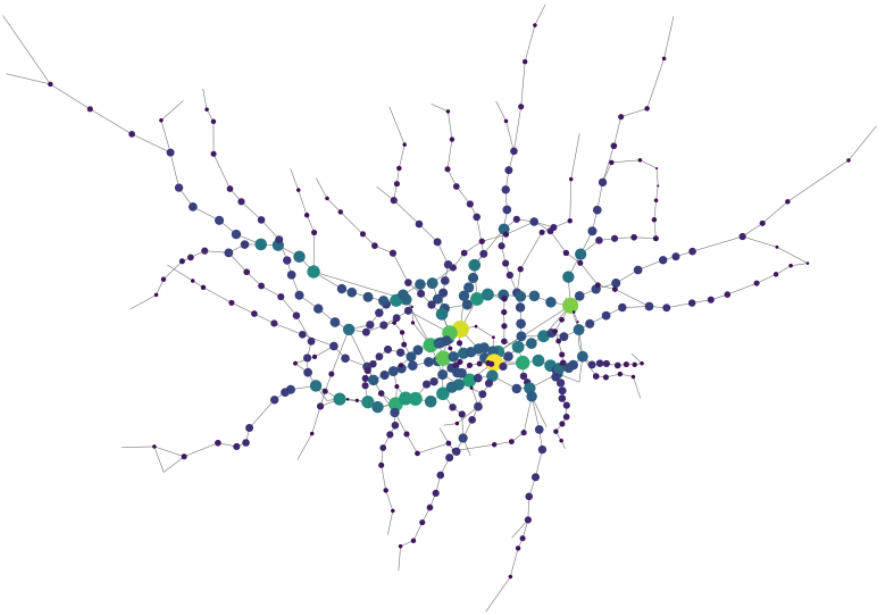

Figure 8: Flow Betweeness Centrality of London Underground

The comparison of the highest-ranked nodes in weighted and unweighted networks for Betweeness reveals differences and overlaps. Bank and Monument, Stratford and King's Cross St. Pancras appearing prominently in both lists, whereas Liverpool Street and Green Park are unique to the unweighted network. Flows can thus alter the importance of certain nodes (Zhou & Wang 2018).

2.2 Impact Measures Transformation in a Weighted Network

Global efficiency is preferred over average shortest path length because it considers all possible paths in a network, not just the shortest ones. This makes it better for understanding the full impact of changes, like removing a node, because it captures how well the network functions as a whole (Wu et al. 2013).

To adjust the global efficiency calculation for a weighted network, you replace the shortest path lengths in the formula with the shortest weighted path lengths, where these lengths factor in the edge weights (e.g., passenger flows). Essentially, this means calculating the shortest path using the weights as distances, and then applying the original efficiency formula with these weighted distances. We will call this "Weighted Network Efficiency" (Latora & Marchiori 2001) (Wu et al. 2013)

$$E_{global} = \frac{1}{N(N-1)} \sum_{i \neq j \in N} \frac{1}{d_{ij}^{w}} \tag{9}$$

- E_{global}: Global efficiency of the network, measuring the average inverse shortest path length across all pairs of nodes.
- N: Total number of nodes in the network.
- i, j: Indices representing distinct nodes in the network.
- d_{ij}^{w}: Shortest path length between node i and node j considering the weights of the edges.

2.3 Node Removal in a Weighted Network

Below we **sequentially** remove the top three nodes based on Betweeness score.

		Weighted		
Removal	Station Removed	Path Distance	Network Efficiency	% Network Connected
0	-	13.545998	0.101256	100
1	Bank and Monument	14.144925	0.096805	99.75
2	King's Cross St. Pancras	15.665529	0.089880	99.50
3	Canada Water	18.158260	0.083136	99.25

Table 11: Sequential Node Removal: Weighted Betweeness Centrality

		Normalised	
Removal	Station Removed	% Change in Path Distance	% Change in Efficiency
1	Bank and Monument	0.011156	0.010461
2	King's Cross St. Pancras	0.027147	0.018066
3	Canada Water	0.040284	0.018995

Table 12: Changes to Weighted Impact Measures

With each station we removed, the network connectivity decreased slightly. Bank and Monument's closure would have the largest impact on passengers as it is the highest ranked station. However, when looking at the impact of each node removal Canada Water's absence notably disrupts passenger flow. Removing it, increases average journey distances by 15.9%, from 15.67 to 18.16. Additionally, network efficiency drops by 7.5% without Canada Water, from 0.090 to 0.083, underscoring its key role in managing passenger flows smoothly across the system.

3 Spatial Interaction Models

We now move into the second half of our analysis. Here, we simulate how passenger flows are impacted by cost hikes and jobs reductions. This section provides an overview of the the different types of spatial interaction models, selects a spatial interaction model and calibrates its parameters and finally uses this calibrated model to simulate the scenarios mentioned above.

3.1 Model's and Calibration

3.1.1 Unconstrained Model

The Unconstrained Model predicts the flow of people between two points or nodes based on size and distance. These models are not limited by the capacity of the destination or the number of people or goods sent from the origin (Batty 2009). It equation is:

$$T_{ij} = k\frac{O_i^{\alpha} D_j^{\gamma}}{d_{ij}^{\beta}} \tag{10}$$

OR

$$T_{ij} = kO_i^{\alpha} D_j^{\gamma} d_{ij}^{-\beta} \tag{11}$$

The above equations define the flow of people or goods T_{ij} between points i and j. Using the emissivity of the Origin, denoted as O, and attractiveness of the Destination, denoted as D (Fotheringham 2001). β refers to the how sensitive the person or good is to travelling marginal distance, α refers to the *emissivity* of the origin. This is the willingness of the population to travel from the destination. γ refers to the attractiveness or *pull* of the destination and

k is a general scaling parameter, representing the size and number of people interacting in the model (Fotheringham 2001).

3.1.2 Singly Constrained Models

Origin-Constrained Model

In a production-constrained model, the total outflows from each origin are fixed. The model is represented as:

$$T_{ij} = A_i O_i D_j^{\gamma} d_{ij}^{-\beta} \tag{12}$$

T_{ij} is the flow of interactions from origin i to destination j. A_i is the origin-specific balancing factor, ensuring that the sum of predicted flows from origin i matches the observed outflows (*Spatial Interaction Models and the Role of Geographic Information Systems* 2006). O_i represents the total observed outflows from origin i. The model predicts flows T_{ij}, adjusting them according to destination attractiveness D_j, distance d_{ij}, and the parameters γ and β (Wilson 1971).

Variables and Parameters

γ is the parameter controlling the influence of the attractiveness of destination j. β: The distance decay parameter, indicating how the interaction between i and j decreases with increasing distance and D_j:

$$D_j = \sum_i T_{ij} \tag{13}$$

A_i is the origin-specific balancing factor is adjusted to ensure that the total outflows from origin i match the observed outflows.

$$A_i = \frac{1}{\sum_j B_j D_j^{\gamma} d_{ij}^{-\beta}} \tag{14}$$

Destination-Constrained Model

$$T_{ij} = D_j B_j O_i^{\alpha} d_{ij}^{-\beta} \tag{15}$$

In an attraction-constrained model, similar to the origin-constrained model, the focus shifts to ensure that the total inflows to each destination are fixed. For this model, a balancing factor B_j is introduced. It is a destination-specific balancing factor, adjusted to ensure that the total inflows to destination j match the observed inflows. (Fotheringham 2001)(Wilson 1971)(*Spatial Interaction Models and the Role of Geographic Information Systems* 2006). It is defined as:

$$B_j = \frac{1}{\sum_i O_i^{\alpha} d_{ij}^{-\beta}} \tag{16}$$

3.1.3 Doubly Constrained Spatial Interaction Model

The doubly constrained model combines both origin and destination constraints. It ensures that both the total outflows from origins and the total inflows to destinations are simultaneously satisfied (*Spatial Interaction Models and the Role of Geographic Information Systems* 2006). This model is articulated as:

$$T_{ij} = A_i O_i B_j D_j^{\gamma} d_{ij}^{-\beta} \tag{17}$$

The doubly constrained model, utilising balancing factors A_i (origin-specific) and B_j (destination-specific), adjusts to align predictions with actual flows, ensuring supply and demand balance. This model overcomes limitations of simpler versions by addressing both origin and destination constraints, reflecting real-world capacities (Wilson 1971)(*Spatial Interaction Models and the Role of Geographic Information Systems* 2006).

3.1.4 Model Selection

Our analysis will use an Origin Constrained Model with exponential decay and Poisson distribution. This model is selected to simulate the morning rush of passenger flows into London's business districts. Exponential decay best represents the sharp decline in commuter numbers over distance compared to an inverse power law common of intercity commuter patterns (Sun et al. 2018). We enhance model precision by adopting a Poisson distribution to capture the probabilistic nature of station flows (Sun et al. 2018).

Using the model above on London Passenger flows we calibrate β as 0.0001435. As a reminder, β measures the decline in travel propensity with distance, is essential for representing the effect of distance on flows. We calculate γ as 0.7259, the parameter controlling the influence of the attractiveness of destination j

$$T_{ij} = A_i O_i B_j D_j^{0.7259} e^{-0.0001435 d_{ij}} \tag{18}$$

These parameters indicate passenger flow between stations is somewhat proportional to origin population size and moderately influenced by destination attractiveness (e.g., job availability), but only mildly affected by distance. The calibrated β value of 0.0001435 reveals low distance sensitivity, suggesting longer travel distances are more acceptable. Our β and γ values show a balanced sensitivity to origin size and destination attractiveness (Liu et al. 2020).

3.2 Scenario Analysis

Below, we assess three scenarios using the Origin Constrained Model defined above.

3.2.1 Scenario A

In the first scenario, we assume Brexit results in a 50% job reduction in Canary Wharf from 58,772 to 29,386. To maintain commuter numbers, we recalculate

destination attractiveness by adjusting Canary Wharf's job count while keeping β: 0.0001435 and γ: 0.7259 constant, reflecting unchanged commuter behaviors despite job distribution shifts. Origin balancing factors A_i were recalculated to align new flows with original outflows from each origin.

Scenario A results show a 50% job cut in Canary Wharf drops its incoming flows by 36.9% from 47,194 to 29,763. This job decrease leads to a network-wide flow redistribution, with 19.47% of station pairs seeing increased flow and only 0.67% of pairs decreased. Overall, the network's flow changes 1.37% on average, showing minimal network impact despite significant reductions at Canary Wharf.

3.2.2 Scenario B1 & B2

Scenario B evaluates the impact of 400% and 900% network-wide edge distances or *costs*. Scenario B1 adjusts the original β value to 0.0007175 (0.0001435 x 5) and Scenario B2 to 0.001435 (0.0001435 x 10). Total commuter flows are maintained by recalculating A_i.

Under increased transport distances, the Underground experiences notable changes in commuter patterns. Scenario B1's 400% distance increase results in a median flow drop of 7 flows per edge and 86.51% of edges experiences a decrease in flows. Scenario B2's 900% increase amplifies these effects, with a median flow drop of 9 flows per edge and 90.95% of edges experiences a decrease in flows

3.2.3 Analysis

The 50% job reduction at Canary Wharf decreased flows, however, the 400% and 900% distance increases more drastically affected commuter patterns, particularly under the 900% increase in Scenario B2. Scenario B2 most significantly redistributed flows, leading to more pairs experiencing decreased flows and a shift toward shorter routes, indicating a substantial change in commuter behavior as passengers sought cost-minimising alternatives.

In Scenario A, 19.47% of station pairs saw increased flows, 79.86% saw no change, and 3.98% saw decreased flows. Scenario B1 showed 9.51% of station pairs with increased flows, 4% saw no change and 86.51% experienced decreased flows. Scenario B2 revealed 5.35% of station pairs with increased flows, 3.70% with no change and 90.95% with decreased flows, highlighting that Scenarios B1 and B2 significantly alter flow distribution more than Scenario A. These figures are illustrated below.

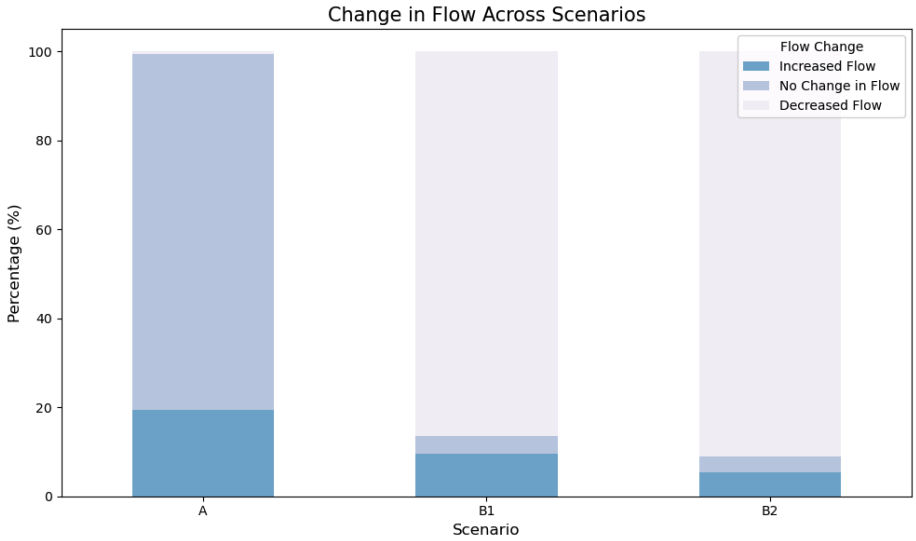

Figure 9: Change in Flows for each Scenario

We now investigate the underlying relationships of how these job cuts and cost increases impact commuter flow and compare these relationship to each other. By understanding the nature of each scenario's impact we highlight *why* a 900% increase impacts flows more than job closures.

Below we plot the change in commuter flows in each scenario.

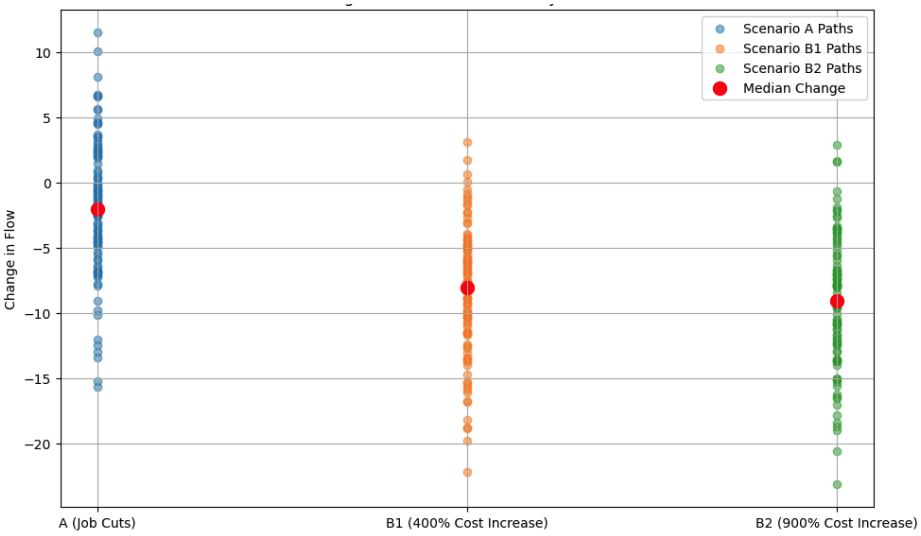

Figure 10: Median Change in Commuter Flow for each Scenario

The median changes across the scenarios progressively decrease, indicating a stronger negative impact on commuter flows as the interventions become more severe (from job cuts to a 900% fare increase). These values illustrate that the proposed cost increases have a more substantial median impact on reducing commuter flows than job cuts:

Scenario	% Change in Network Flows
A	-1.17
B1	-7.32
B2	-8.87

Table 13: Median Change in Network Flow for Each Scenario

By comparing the standard deviations, we can comment on the consistency of the impact across the network. A higher standard deviation indicates more variability in how different station pairs are affected, while a lower standard deviation suggests a more uniform impact. The increasing standard deviation from Scenario A to B2 indicates that the impacts of the cost increases are more severe on average.

Scenario	Standard Deviation
A	4.42
B1	4.58
B2	4.88

Table 14: Standard Deviation of Each Scenario's Median Flow Distribution

Additionally, by examining the percentage of station pairs that experienced decreases in flows beyond a 10% threshold, we can understand the severity of each scenario's impact. A higher percentage indicates a more severe impact across the network.

Scenario	Beyond -10%
A	0
B1	33.33%
B2	40%

Table 15: % of station pairs that experienced -10% or greater Change in flows

This shows that while there are no changes exceeding a 10% decrease in Scenario A, a significant portion of the changes in Scenarios B1 and B2 do. In Scenario B2, 40% of the changes surpass this threshold, highlighting the severe negative impact on commuter flows.

In conclusion, the analysis indicates that these *cost* increases have a more severe negative impact on commuter flows than job cuts at Canary Wharf. As we move from job reductions to a 900% *cost* increase, the median flow change

becomes increasingly negative, highlighting a stronger deterrent to commuting. Moreover, the significant proportion of changes in Scenarios B1 and B2 that exceed a -10% threshold—absent in Scenario A—emphasises the more pronounced negative impact of fare increases on public transportation's accessibility and attractiveness.

Analysis in Python

References

Batty, M. (2009), Urban Modeling, *in* R. Kitchin & N. Thrift, eds, 'International Encyclopedia of Human Geography', Elsevier, Oxford, pp. 51–58.
URL: *https://www.sciencedirect.com/science/article/pii/B9780080449104010920*

British Transport Police (n.d.), 'London bombings of 2005'.
URL: *https://www.btp.police.uk/police-forces/british-transport-police/areas/about-us/about-us/our-history/london-bombings-of-2005/*

Derrible, S. (2012), 'Network Centrality of Metro Systems', *PLOS ONE* **7**(7), e40575. Publisher: Public Library of Science.
URL: *https://journals.plos.org/plosone/article?id=10.1371/journal.pone.0040575*

Esposito Amideo, A., Starita, S. & Scaparra, M. P. (2019), 'Assessing Protection Strategies for Urban Rail Transit Systems: A Case-Study on the Central London Underground', *Sustainability* **11**(22), 6322. Number: 22 Publisher: Multidisciplinary Digital Publishing Institute.
URL: *https://www.mdpi.com/2071-1050/11/22/6322*

Fotheringham, A. S. (2001), Spatial Interaction Models, *in* N. J. Smelser & P. B. Baltes, eds, 'International Encyclopedia of the Social & Behavioral Sciences', Pergamon, Oxford, pp. 14794–14800.
URL: *https://www.sciencedirect.com/science/article/pii/B0080430767025195*

Latora, V. & Marchiori, M. (2001), 'Efficient Behavior of Small-World Networks', *Physical Review Letters* **87**(19), 198701. Publisher: American Physical Society.
URL: *https://link.aps.org/doi/10.1103/PhysRevLett.87.198701*

Liu, Y., Tang, M., Wu, Z., Tu, Z., An, Z., Wang, N. & Li, Y. (2020), 'Analysis of passenger flow characteristics and their relationship with surrounding urban functional landscape pattern', *Transactions in GIS* **24**(6), 1602–1629. _eprint: https://onlinelibrary.wiley.com/doi/pdf/10.1111/tgis.12665.
URL: *https://onlinelibrary.wiley.com/doi/abs/10.1111/tgis.12665*

Lucy Rodgers, Salim Qurashi & Steven Connor (2015), '7 July London bombings: What happened that day?', *BBC News* .
URL: *https://www.bbc.com/news/uk-33253598*

Napitupulu, H., Carnia, E., Anggriani, N. & Supriatna, A. K. (2021), 'Centrality measures in transportation networks for Unpad campus route', *Journal of Physics: Conference Series* **1722**(1), 012063. Publisher: IOP Publishing.
URL: *https://dx.doi.org/10.1088/1742-6596/1722/1/012063*

Spatial Interaction Models and the Role of Geographic Information Systems (2006), *in* M. M. Fischer, ed., 'Spatial Analysis and GeoComputation: Selected Essays', Springer, Berlin, Heidelberg, pp. 29–42.
URL: *https://doi.org/10.1007/3-540-35730-0*$_3$

Stamos, I. (2023), 'Transportation Networks in the Face of Climate Change Adaptation: A Review of Centrality Measures', *Future Transportation* **3**(3), 878–900. Number: 3 Publisher: Multidisciplinary Digital Publishing Institute.
URL: *https://www.mdpi.com/2673-7590/3/3/49*

Sun, J., Staab, S. & Karimi, F. (2018), Decay of Relevance in Exponentially Growing Networks, *in* 'Proceedings of the 10th ACM Conference on Web Science', WebSci '18, Association for Computing Machinery, New York, NY, USA, pp. 343–351.
URL: *https://doi.org/10.1145/3201064.3201084*

Vragović, I., Louis, E. & Díaz-Guilera, A. (2005), 'Efficiency of informational transfer in regular and complex networks', *Physical Review E* **71**(3), 036122. Publisher: American Physical Society.
URL: *https://link.aps.org/doi/10.1103/PhysRevE.71.036122*

Wilson, A. G. (1971), 'A Family of Spatial Interaction Models, and Associated Developments', *Environment and Planning A: Economy and Space* **3**(1), 1–32. Publisher: SAGE Publications Ltd.
URL: *https://doi.org/10.1068/a030001*

Wu, Z., Hou, B. & Zhang, H. (2013), 'Efficiency of transportation on weighted extended Koch networks', *The European Physical Journal B* **86**(10), 405.
URL: *https://doi.org/10.1140/epjb/e2013-40246-5*

Ye, Y., De Moortel, K. & Crispeels, T. (2020), 'Network dynamics of Chinese university knowledge transfer', *The Journal of Technology Transfer* **45**(4), 1228–1254.
URL: *http://link.springer.com/10.1007/s10961-019-09748-7*

Zhang, Y., Marshall, S. & Manley, E. (2019), 'Network criticality and the node-place-design model: Classifying metro station areas in Greater London', *Journal of Transport Geography* **79**, 102485.
URL: *https://www.sciencedirect.com/science/article/pii/S0966692319300377*

Zhou, Y. & Wang, J. (2018), 'Efficiency of complex networks under failures and attacks: A percolation approach', *Physica A: Statistical Mechanics and its Applications* **512**, 658–664.
URL: *https://www.sciencedirect.com/science/article/pii/S0378437118310355*